Ultrasound in Med. & Biol., Vol. 31, No. 9, pp. 1265–1277, 2005

0301-5629/05/$–see front matter

ELSEVIER

doi:10.1016/j.ultrasmedbio.2005.05.005

● *Original Contribution*

MICROFLUIDIC SONICATOR FOR REAL-TIME DISRUPTION OF EUKARYOTIC CELLS AND BACTERIAL SPORES FOR DNA ANALYSIS

THEODORE COSMO MARENTIS,*† BRENDA KUSLER,‡ GOKSEN G. YARALIOGLU,† SHIJUN LIU,† EDWARD O. HÆGGSTRÖM,†§ and B. T. KHURI-YAKUB†

*Harvard Medical School, Boston, MA, USA; †Edward L. Ginzton Laboratory and ‡Department of Biological Sciences, Stanford University, Stanford, CA, USA; and §Department of Physics, University of Helsinki, Helsinki, Finland

(*Received* 9 *December* 2003, *revised* 5 *May* 2005, *in final form* 24 *May* 2005)

Abstract—Biologic agent screening is a three-step process: lysis of host cell membranes or walls to release their DNA, polymerase chain reaction to amplify the genetic material and screening for distinguishing genetic signatures. Macrofluidic devices commonly use sonication as a lysis method. Here, we present a piezoelectric microfluidic minisonicator and test its performance. Eukaryotic human leukemia HL-60 cells and *Bacillus subtilis* bacterial spores were lysed as they passed through a microfluidic channel at 50 μL/min and 5 μL/min, respectively, in the absence of any chemical denaturants, enzymes or microparticles. We used fluorescence-activated cell sorting and hematocytometry to measure 80% lysis of HL-60 cells after 3 s of sonication. Real-time polymerase chain reaction indicated 50% lysis of *B. subtilis* spores with 30 s of sonication. Advantages of the minisonicator over macrofluidic implementations include a small sample volume (2.5 μL), reduced energy consumption and compatibility with other microfluidic blocks. These features make this device an attractive option for "lab-on-a-chip" and portable applications. (E-mail: theodore_marentis@hms.harvard.edu) © 2005 World Federation for Ultrasound in Medicine & Biology.

Key Words: **Ultrasound, Sonication, Piezoelectric, Bioeffect, Lysis, Microfluidic, Lab-on-a-chip.**

INTRODUCTION

A variety of fields, such as medical diagnostics or "lab-on-a-chip," can greatly benefit from rapid, on the spot identification of biologic agents. Detection can be accomplished either by DNA hybridization methods (Hianik et al. 2000) that require a large number of DNA copies and, thus, a polymerase chain reaction (PCR) step, or quantitative real-time PCR (RTPCR) (Belgrader et al. 1999). In either case, fast and reliable PCR takes place when cellular hosts are disrupted and their intracellular DNA is made available in solution to interact with the polymerase enzyme. This makes cell lysis a necessary step in the detection process.

A variety of cell lysing methods exist, such as physical, thermal, chemical, enzymatic or mechanical (Kuske et al. 1998; More et al. 1994), which, however, can be too labor-intensive for timely on-site applications (Chandler et al. 2001). Often, they require additional consumables with a certain shelf-life. These consumables may further complicate subsequent PCR and detection steps by altering chemical conditions such as pH, or by inhibiting the necessary molecular interactions (Chandler et al. 2001). To overcome these difficulties, research has focused on sonication or the use of ultrasound (US) to disrupt cellular membranes and spore coats (Belgrader et al. 1999; Chandler et al. 2001; Taylor et al. 2001).

To the authors' knowledge, no comprehensive study is available on threshold pressures required to lyse spores and cells. As reported in the literature, portable sonication implementations developed to date lie in the macrofluidic realm (Belgrader et al. 1999; Chandler et al. 2001; Taylor et al. 2001; Kawai and Iino 2003; Feril et al. 2003; Miller et al. 2003). One disadvantage with these systems is the length of the tubing required to connect the components. Use of microbeads to enhance bacterial spore lysis is also common (Belgrader et al. 1999; Taylor et al. 2001). These beads, however, have to be washed to remove adhered DNA, which complicates the process. Although successful in lysing eukaryotic cells and bacterial spores,

Address correspondence to: Theodore Cosmo Marentis, 107 Avenue Louis Pasteur, Box 239 Vanderbilt, Harvard Medical School, Boston, MA 02115 USA. E-mail: theodore_marentis@hms.harvard.edu

size and energy consumption preclude macrofluidic implementations from delivering a truly portable screening device (NASA Fundamental Space Biology homepage, available at: http://fundamentalbiology.arc.nasa.gov/EP/EPpres2.html).

Unfortunately, *Bacillus anthracis* (anthrax) has recently re-emerged as a potential threat in the hands of the wrong people. Its spores are easily cultivated *en masse*, stored for decades in their vegetative state and can be easily aerosolized (Inglesby et al. 1999). This has strengthened efforts to improve the speed and specificity of available biologic agent detection methods, as well as the portability of the testing equipment (DARPA, Defense Advanced Research Project Agency homepage, available at: http://www.darpa.mil/MTO/bioflips). To ensure specificity, detection methods screen for genetic signatures that confer toxicity to anthrax (Read et al. 2003; Ivanova et al. 2003), which leads back to the problem of cell lysis.

Meanwhile, the concept of "lab-on-a-chip" is evolving (Knight 2002; Anderson and van den Berg 2003). A variety of new microelectromechanical and microfluidics implementations are being developed, such as electro-osmotic pumps (Zeng et al. 2001), ultrasonic mixers (Yaralioglu et al. 2004), small PCR chambers (Kopp et al. 1998; Lagally et al. 2001; Sun et al. 2002) and electrical readout DNA arrays (Umek et al. 2001; Patolsky et al. 2001; Thewes et al. 2002). These microfluidic blocks can be patterned on silicon and cascaded next to each other. This allows complex biologic and chemical experiments to be performed on a computer-controlled chip, with minute sample volumes, thus reducing reagent and labor costs. Currently, no efficient on-a-chip lysis block exists. Lysing has so far been performed macrofluidically, comprising a bottleneck for any "lab-on-a-chip" assay (Chandler et al. 2001).

We present a microelectromechanical-based piezoelectric microfluidic minisonicator operated in the 380 MHz range to fill this need for a miniaturized lysing device. The device lyses cells in the absence of chemical, biologic or microparticle agents in a continuous manner as they flow through a 50-μm channel. This allows for real-time continuous monitoring applications. We tested the minisonicator with eukaryotic HL-60 cells that lack a cell wall and then proceeded to vegetative *B. subtilis* bacterial spores, which are considered to be difficult to lyse (Taylor et al. 2001). To our knowledge, this is the first microfluidic device that disrupts cells with US.

MATERIALS AND METHODS

Device design and fabrication

We have developed a microfluidic channel with integrated transducers (Jagannathan et al. 2001, 2003a, 2003b). The geometry of the device is shown in Fig. 1. The device is composed of two parts, the channel and the transducers. The channel was fabricated on a glass substrate, whereas the transducers were fabricated on a quartz substrate. The substrates are 20 $\times$ 25 mm in size. Glass was chosen for the channel material because it is transparent and can be micromachined. The channel was formed by wet-etching the glass substrate in a 50:1 hydrofluoric acid solution (Gallade Chemical Inc., Escondido, CA, USA). A 0.5-μm layer of photolithographically patterned polysilicon was used as a masking layer. The dimensions of the channel were 10 mm in length, 500 μm in width and 500 μm in depth. Hence, the cross-section was 0.25 mm^2, and the volume was 2.5 mm^3, giving a flow-velocity of 4 mm/s at 1 μL/s flow. These dimensions should be compared with those of 10 μm by radius HL-60 cells (van Dujin et al. 1998) and 0.7 μm by diameter and 2 to 6 μm by length *B. subtilis* spores (Janosi et al. 1998).

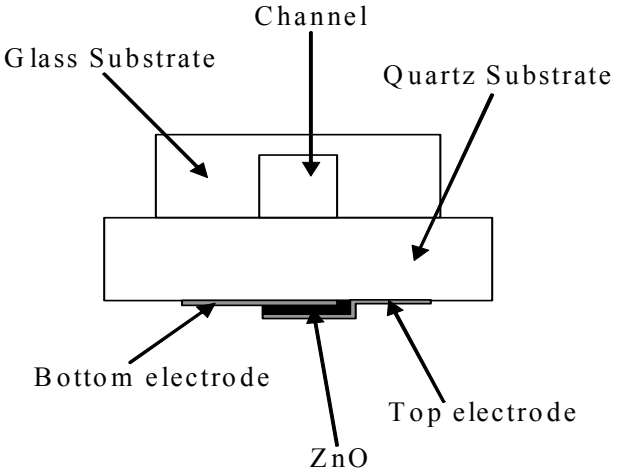

Fig. 1. Cross-section of the microfluidic channel.

The piezoelectric transducers used in our experiments were integrated onto the channel floor by depositing a layer of zinc oxide between two layers of gold on a quartz substrate. Quartz was chosen as a substrate material because of its low loss coefficient for acoustic waves. Figure 2 describes the fabrication steps of the transducer. First, a 0.1-μm film of gold was sputtered and patterned over a glass substrate to serve as one of the electrodes of the transducer (steps 1, 2). This step was followed by deposition of 8 μm of zinc oxide by means of a magnetron sputtering technique (step 3) (Khuri-Yakub et al. 1981) using a shadow mask. Finally, another 0.1-μm thick layer of gold was deposited and patterned using lift-off to serve as the top electrode of the transducer (steps 2, 4, 5, 6). The size of each of the nine piezoelectric transducers was 500 μm by 500 μm, leading to a 45% coverage of the channel floor. The trans-

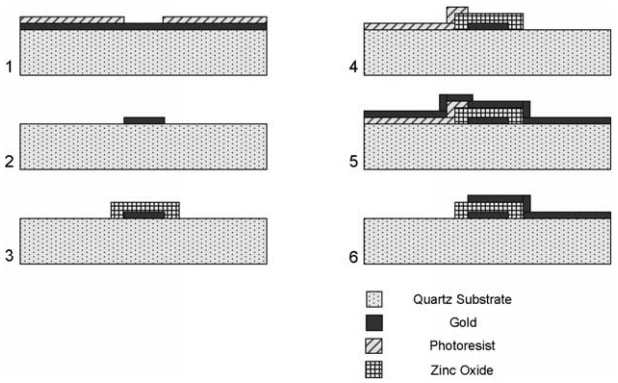

Fig. 2. Fabrication steps for the PZT element.

ducers were 200 μm apart. The theoretical thickness resonance of the transducer, calculated using the Krimholtz–Leedorn–Matthaei (KLM) model (Kino 1987), was 361 MHz. This high frequency also indicates that cavitation probably plays an insignificant role, whereas heating caused by absorption and translation, or shear forces caused by acoustic radiation pressure, could be significant lysing mechanisms.

Finally, the device was assembled by gluing (5 min epoxy, ITW Devcon, Danvers, MA, USA) the channel onto the opposite side of the substrate to that which holds the transducers. The channel was aligned with the transducers, as shown in Fig. 1. The fluid inlet and outlet tubing passed through 0.8-mm diameter holes drilled in the glass substrate. The fabricated device is shown in Fig. 3.

The transducers, impedance-matched to 50 Ω with an LC matching circuit, were driven by a sinusoidal source in the 360-MHz range in the experiments. A continuous signal was applied because sonolysis increases with increased pulse duration and duty factor (Chen et al. 2003). The frequency was chosen so that one of the longitudinal resonances of the substrate-piezo combination would be excited. This maximized the acoustic power coupled into the liquid filling the microfluidic channel. Because of the high frequency, the acoustic amplitude attenuated by 31 dB, mostly as a result of heat dissipation, during one round trip in the channel (0.03 dB/μm). This was approximately half the channel height. Therefore, we expect no strong standing wave formation in the channel.

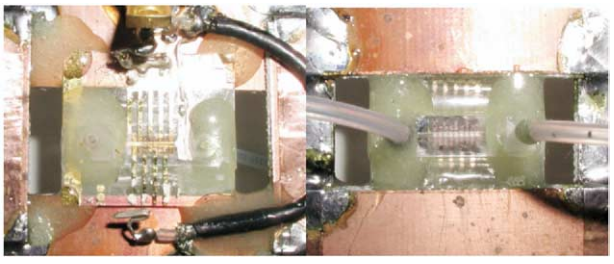

Fig. 3. Microfluidic device with integrated transducers. (a) Channel side, and (b) transducer side.

Eukaryotic HL-60 cell preparation

We maintained HL-60 cells (strain human, caucasian promyelocytic, ATCC CCL-240) in logarithmic growth in RPMI 1640 (Gibco; cat. 31800 BRL, Grand Island, NY, USA) supplemented with 20% heat-inactivated fetal bovine serum (Gibco), 55 μM β-mercaptoethanol (1000x stock; Gibco), 2 mM glutamine, 100 U/mL penicillin and 100 mcg/mL streptomycin (Gibco). We harvested the cells by centrifugation at 400 *g*. Cell pellets were resuspended and washed 3 times in 1x phosphate-buffered saline (PBS; Gibco). Cells were then counted by a hemacytometer (Hausser Scientific, Horsham, PA, USA) and their presonication viability, defined as the number of trypan blue negative cells in the total cell count, was determined with 0.4% trypan blue in 0.85% saline (Gibco).

Initial cell viability averaged 90% $\pm$ 2.8% and we resuspended the cells at a final concentration of $\approx 5 \times 10^5$ cells/mL PBS for use in the experiments. To reduce time-dependent cell death and aging effects, cells were harvested immediately before use and then vortexed for 2 s before loading into a syringe. The HL-60 cells were maintained in their most predictable growth phase (mid-logarithmic, 40% G0/G1, 20% S 40% G2/M) to make the impact of the sonication as distinguishable as possible and to keep the cell age variation small (Kuske et al. 1998). This meant that we did not take advantage of the fact that older cells are less tolerant of shear stress than are younger cells. The doubling time of the cells was $\approx$ 12 h.

To determine how much heat the minisonicator generated, we conducted heating tests before the lysing experiments. Sonication-induced heating was measured with a Fluke 2190A thermometer using a 125-μm diameter chromel-alumel thermocouple (CHCO-0005, Omega Engineering, Stamford, CT, USA). During a 33-dBm sonication test, the temperature in the channel increased from 20°C to 70°C with 5 μL/min flow and from 20°C to 65°C with 50 μL/min flow. This flow rate corresponds to a 3-s residence time. The 90% thermal rise-time of the channel was 100 s. After this, the channel reached thermal equilibrium with its surroundings. Hence, any subsequent sonication that heats the channel does not force the narrowband lead zirconate-titanate (PZT) transducer off-resonance.

The elevated temperature caused evaporation at the exit of the orifice, which reduced the volume of sample recovered. To minimize evaporation losses, we imple-

mented a condenser element by trapping the exit tubing between a copper plate cold finger and an ice pack, maintaining the temperature of the sample leaving the channel at 4°C. This allowed us to recover approximately 98% of each sample's original volume.

HL-60 cell lysis using the minisonicator

To maximize cell viability, the cells remained outside the culture medium for a maximum of 50 min and all data were collected within this time frame. An even distribution of the HL-60 cells in suspension was ensured by pipetting after vortexing. The cells were loaded on plastic Monoject 12-mL syringes and passed *via* Cole Parmer (Tygon 3350 silicone 1/32 × 3/32) tubes through the minisonicator channel at a constant flow rate of 50 μL/min. This corresponded to ≈ 400 cells/s at a concentration of 480 cells/μL. The flow was controlled by a Harvard Instruments PHD 2000 programmable syringe pump (Harvard Apparatus, Holliston, MA, USA). The resident time of a cell in the channel was 3 s and the treatment time was 1.35 s, corresponding to 0.15 s per transducer.

The minisonicator was excited with a continuous sinusoidal signal from an 8656B (Hewlett Packard, Palo Alto, CA, USA) signal generator at 384.2 MHz, amplified by a 20-dB power amplifier (Mini-Circuits ZHL-2-50P3, Brooklyn, NY, USA). We tested lysis at eight consecutive power levels between 15 and 23 dBm, corresponding to maximally 4.5 V_{peak} across the PZT elements matched to 50 Ω (0.2 W). The maximum acoustic intensity in front of a transducer was, thus, 8.84 W/cm^2, with a predicted output pressure p_o of 0.52 MPa.

We collected three 750-μL samples per power level, washing with 3 mL of PBS between samples and with 5 mL of PBS between power levels. This ensures the cleanliness of the channel and the passivation of the channel surfaces, namely, the inactivation of dangling chemical bonds on the substrate surface, rendering it inert. Cleanliness was assessed by microscopy, using a magnification of 45x and a field-of-view of 16 mm^2, to verify that no visible cell debris remained in the channel.

Quantifying lysis by FACS and hematocytometry

The samples were collected in 12 × 75 polystyrene fluorescence-activated cell sorter (FACS) tubes (Falcon #35-2058, BD Bioscience, Palo Alto, CA, USA). To 100 μL of the main sample (≈ 5×10^4 cells), we added 100 μL trypan blue (Gibco), a membrane-impermeable dye that only stains dead cells. Using a hemacytometer (Hausser Scientific) with a field of view ≈ 0.3 cm^2 and a magnification of 100x, we counted the number of viable (trypan-blue negative) and dead (trypan-blue positive) cells in each of the four corner squares of the chamber. The numbers were averaged, multiplied by a dilution factor of 2 to compensate for the addition of 1:1 phenyl-methyl blue and then by 10^4 (a manufacturer-provided value) to produce the concentration of live and dead cells in a sample. We performed this process after each treatment, as well as each time we took cells out of the culture.

In the remaining sample, we added 2 μL of 10 mg/mL propidium iodide (PI, Sigma–Aldrich, St. Louis, MO, USA), a membrane-impenetrable fluorescent dye that stains dead cells, and analyzed the sample using a Beckman-Coulter EPICS XL-MCL FACS flow cytometer (Beckman-Coulter Inc, Miami, FL, USA), exciting the PI at 488 nm. The FACS was set to collect 10,000 events per run.

Cell viability was determined by PI exclusion (monitoring fluorescent emission at 575 nm) of particles in the size range 0.5 to 5 μm. Plots of PI fluorescence intensity at 575 nm vs. event count, corresponding to the passage of a particle with size larger than the forward scatter size detection threshold, revealed the percent of cells absorbing PI (Fig. 4, first column). From 2-D plots of the forward light scatter (FSC) vs. side light scatter (SSC), we determined the amount of structural damage induced by the sonication (Fig. 4, second column).

We used two different forward scatter detection thresholds, one at FS10 that detects fragments larger than 0.5 μm and one at FS94 that detects fragments larger than 5 μm, to allow us to monitor events related to particles within the 0.5 to 5 μm size range. FS10 was useful in accounting for cell debris resulting from sonication. The effect of mere flow through the channel was assessed by flowing cells through at 50 μL/min with no electrical power applied to the transducer elements.

Spore preparation and lysis using the minisonicator

ATCC 9372 *B. subtilis* var. *niger* spores in water suspension at a concentration of 1.8×10^6 spores/mL were purchased from the American Tissue Culture Collection and stored at 4°C. We first washed the minisonicator channel with 1 mL of 99% ethanol and 5 mL of distilled water. We then shook the spore vial thoroughly to obtain an even spore distribution in suspension at a concentration of 1800 spores/μL. We fully loaded a 250-μL, 2.304-mm diameter Gastight #1725 syringe (Hamilton Co., Reno, NV, USA) with 450,000 spores. A PHD 2000 programmable syringe pump (Harvard Apparatus, Holliston, MA, USA) pushed the spores through the channel at a constant flow of 5 μL/min, corresponding to 150 spores/s. Hence, each spore remained in the channel for 30 s, corresponding to 13.5 s over the ultrasonic transducers or 1.5 s per transducer.

To ensure maximum electric power coupling to the piezo elements, we added a matching series inductor of 0.66 mH to the minisonicator for the spore experiments

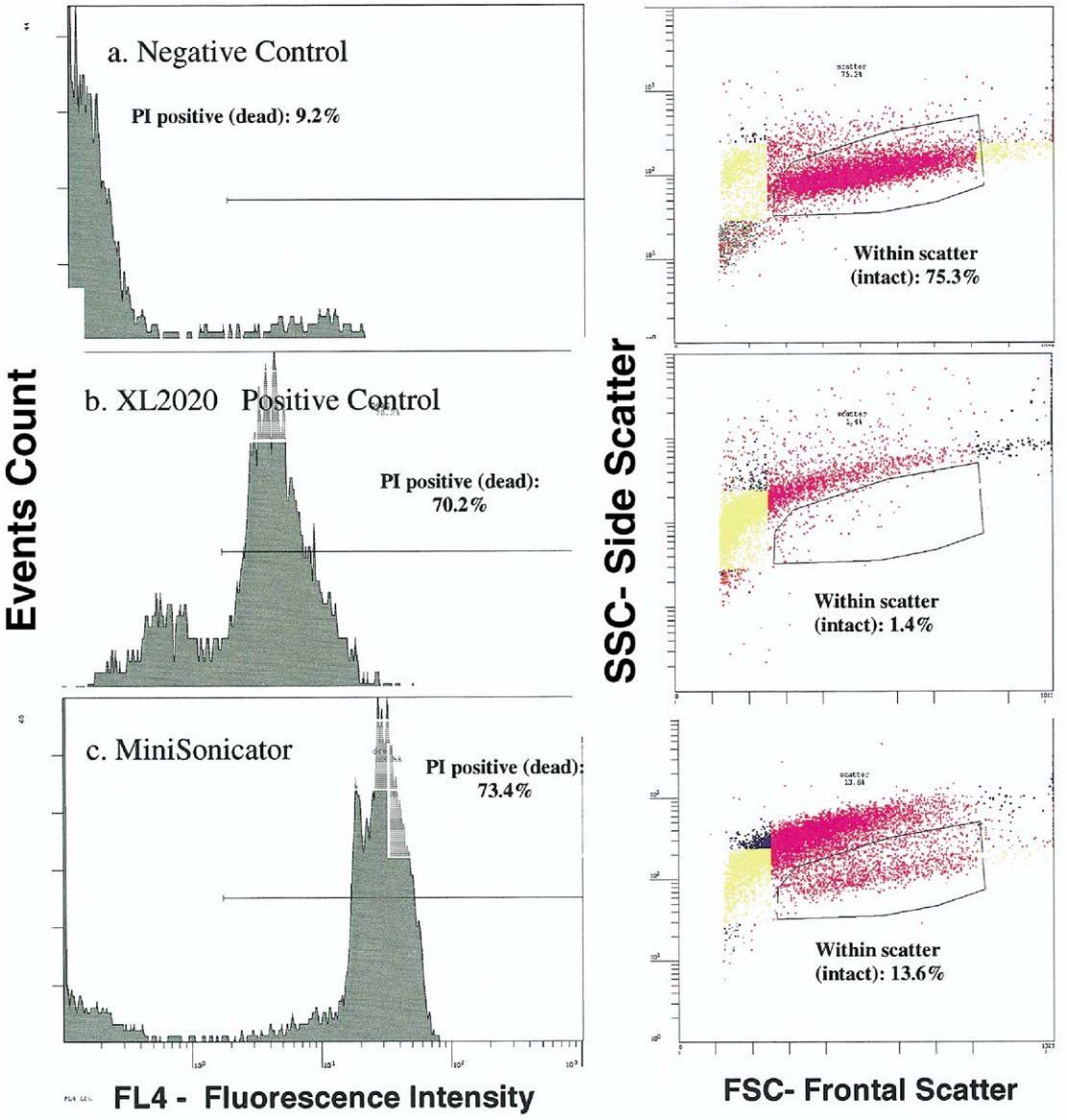

Fig. 4. (left) Fluorescence intensity vs. events count demonstrating PI uptake by dead cells in (a) negative controls, (b) positive controls and (c) samples treated with the microsonicator. (right) FSC- frontal scatter vs. SSC side-scatter plots showing membrane damage and change in geometry; (a), (b) and (c) same as on left. All experiments shown were gated at FS94.

only. This made the transducers resonate at 367.377 ± 0.173 MHz (3 dB band width) with a 0.2% power-loss because of electrical mismatch. At the resonance frequency, a total of 30 dBm of power was delivered. This corresponds to 10.0 V_{peak} across each of the matched 50 Ω PZT elements (1 W). The maximum acoustic intensity in front of a transducer was, thus, 44.4 W/cm^2, corresponding to a pressure p_o of 1.15 MPa.

Positive controls by XL-2020 macrosonication

We used a 550 W sonicator ultrasonic processor XL-2020 macrosonicator (Misonix, Farmingdale, NY, USA) with a 4-mm diameter tip to create positive controls to compare the performance of the minisonicator with that of a standard lysing procedure. Samples were pipetted in 1.7 mL Eppendorf tubes (USA Scientific, Woodland, CA, USA) placed in an ice bath. The macrosonicator tip was in direct contact with the sample and no beads or other microparticles were used. We operated the sonicator at 20 kHz and coupled 1% (5.5 W) of the total power into the medium, as measured by the difference in electrical powers consumed when operating the device in air and in water. Here, we assumed 95% conversion efficiency at resonance. The acoustic inten-

sity was, thus, 41.6 W/cm^2, corresponding to 0.79 MPa. The eukaryotic HL-60 cells were sonicated for 30 s (Fig. 4b), and the spores received 5 min of intermittent treatment, with 30 s of sonication separated by 30-s intervals of inactivity, to allow for cooling of the sample. We set this method to be the "gold standard," assuming that the vigorous macrosonicator treatment lysed the majority of the cells in the sample.

Real-time PCR quantification

We performed RTPCR analysis on a BioRad iCycler (Bio-Rad, Hercules, CA, USA) calibrated with a proprietary well-factor plate mix (Biorad) to determine the sporocidal effect of sonication. Each 200μL reaction aliquot contained 10 μL sample DNA and 10 μL master mix, so that the final reaction conditions included 1x buffer II with Stoffel fragments, 3 mM $MgCl_2$, 0.1 units/mL AmpliTaq polymerase (Applied Biosystems, Foster City, CA, USA), 0.2 mM of each primer (left primer 5′TGATCTTAGTTGCCAGCAT TCAGTT3′ right primer 5′TCTGTCCATTGTAGCACG TGTGTAG3′), 0.125 mM dNTP, 1%$_{vol.}$ phenyl-methyl-sulfonyl-fluoride (PMSF, Sigma-Aldrich) and 0.25x Syber green (Molecular Probes, Eugene, OR, USA). Thermal cycling started with a 5-min hold phase at 95°C followed by 40 cycles of denaturation at 94°C, annealing at 64°C and extension at 72°C, each step lasting 30 s.

The master mix was prepared fresh before every RTPCR experiment. We undertook three consecutive experiments, one with four replications per sample and two with eight replications per sample. In the first experiment, we used three positive controls, 1:4, 1:40 and 1:400 serial dilutions of the spores treated with the macrosonicator. The estimated number of spores in the samples was 4.5×10^5, 4.5×10^4 and 4.5×10^3 spores/mL, respectively. We also included a negative control using a 1:10 dilution of untreated spores in water and a 1:10 dilution of spores treated with the minisonicator.

In the second and third experiments, the positive controls were 1:10, 1:40 and 1:100 serial dilutions of spores treated with the ultrasonic processor XL-2020 horn, estimated to correspond to 1.8×10^5, 4.5×10^4 and 1.8×10^4 spores/mL, respectively. We also tested three negative controls. These were 1:10 dilution of untreated spores, 1:10 dilution of untreated spores containing 1%$_{vol.}$ PMSF in water and a 1:10 dilution of a sample treated with the minisonicator.

In two separate experiments, we weighed the effects of flow on our positive and negative controls. In the first experiment, we compared a 1:10 dilution of sonicated spores treated with the XL-2020 macrosonicator that had passed through the channel with a similar sample that had not. We verified complete sample recovery and confirmed the minimal effect of flow on the positive controls. In a second experiment, we measured the effect of flow-induced shear stress damage on the negative controls. We compared a 1:10 dilution with untreated spores to a similar solution that had passed through the channel at 5 μL/min. Flow did not impact on either the positive or the negative controls.

Data analysis

Counting chamber microscopy data. We established a negative control baseline by averaging all percentages of viable cells before treatment. We attempted to establish a positive control baseline by counting the cells after treating them with the XL-2020 macrosonicator. However, the number of cells counted was just a few per counting chamber and too small to bear statistical significance, allowing us to approximate the positive control baseline to zero cells. Three independent data points were collected at each of the eight power levels and averaged.

FACS data. We used the FACS gated at FS10 and FS94 and analyzed three untreated samples to serve as negative controls. On the FSC vs. SSC plot, we defined a region around the viable cell population bounded by channel numbers $300 < \text{FSC (size)} < 900$ and $30 < \text{SSC (granularity)} < 500$. We then let the EXPO counter software (Coulter) calculate the percentage of total events within that region (*i.e.*, number of cells in region/total number of events 2-D plot times 100). This value (viable/total) established a baseline for the maximum number of viable cells and established our negative controls (Fig. 4b, second column). For every power level, we averaged the percentages from the three parallel samples, divided by the baseline value and multiplied by 100 to reach a final percent of viable cells.

To establish a PI reference, we used cells immediately postharvest and set markers on the FACS screen at the peak of PI positive (*i.e.*, dead/dying cells) and at that of PI negative (*i.e.*, viable cells). The marker was then left in place to act as a reference to determine subsequent marker shifts that indicated death/membrane compromise, or complete cell lysis (Fig. 4a, first column).

We assessed the effects of mere flow with a two-sided heteroscedastic *t*-test that determines if two populations come from the same sample. We ran the test at the 0.05 α level and compared the cell population that had passed through the channel with the negative controls.

Real-time PCR data. The basic PCR equation, $X_n = mX_o(E)^n$, provides the threshold cycle to DNA content function Ct (DNA) (Belgrader et al. 2003). Here, E is the amplification efficiency (maximally 2 ×/cycle), X_o is the initial DNA concentration, X_n is the concentration after n cycles and m is the number of sites that are copied on the

gene. Therefore, each 1/*a* dilution should theoretically increase the Ct number by $\log_{10}(a)/\log_{10}.(mE)$, or $\delta Ct > \log_{10}(10)/\log_{10}(24) = 0.73$ in our case, for a 10-fold dilution. In practice, one expects δCt to be two to three cycles per 10-fold dilution (Belgrader et al. 2003). An estimate of the effective amplification efficiency, $mE = 1.87$, was obtained from the plot of mean Ct value vs. spore concentration in the positive controls. By comparing the difference in mean Ct value for an unsonicated sample with the 1:10 positive control, we estimated the fraction of amount of extracellular DNA to 0.5‰ of the DNA content within the cell.

We based our RTPCR detection method on the principle that the more damage the sonicator induces, the more DNA the spores release and the earlier we see the threshold cycle (Ct) of the sample's RTPCR curve. To increase the robustness of our analysis, we defined the threshold cycle (Ct) in two different ways. These were: 1. the point in time at which the signal enters the linear phase of the logarithmic curve (Ct_{low}) and 2. the inflexion point in the linear phase of the sigmoid growth curve (Ct_{high}). We began by averaging the four growth curves per sample of the first experiment and discarded one, corresponding to a 3.6% trimmed average (see Discussion section). For the second and third experiments, we averaged the eight growth curves per sample and discarded 12, corresponding to a 12.5% trimmed average. The averaged data from experiment 3 are shown in Fig. 5.

We determined the Ct_{low} and Ct_{high} for each of the averaged growth curves. We graphed, for calibration purposes, the concentration of the three positive controls vs. their respective Ct values, separately for Ct_{low} and Ct_{high}, and curve-fit the data both linearly (Fig. 6a) and logarithmically (Fig. 6b). This produced a linear and a logarithmic mathematical formula for Ct_{low} and, similarly, for Ct_{high}, of the form Ct = F(x), where x is the percent of DNA available. We entered the Ct value of the sample treated with our minisonicator into the formula and solved for DNA concentration. The percent of available DNA correlates with the percentage of compromised spores that allowed their DNA to leak outside the spore.

For instance, if the Ct of our sample approached that of the 1:10 dilution control and our sample dilution also was 1:10, then we released almost 100% of available DNA. If the sample Ct was closer to the 1:40 dilution control, then we only released 25%. We finally plotted this estimate of number of lysed spores against threshold cycle on the same plot as the serial dilutions controls (Fig. 6).

The SD of the Ct was converted to SD along the concentration axis using the aforementioned mathematical relations. Using a bootstrapping (Rothery et al. 1997) procedure on Matlab (Mathworks Inc., release 13), we averaged Ct_{low} and Ct_{high} separately across all experiments. Finally, we averaged the averages of Ct_{low} and Ct_{high} across all three experiments to arrive at a final lysis percentage.

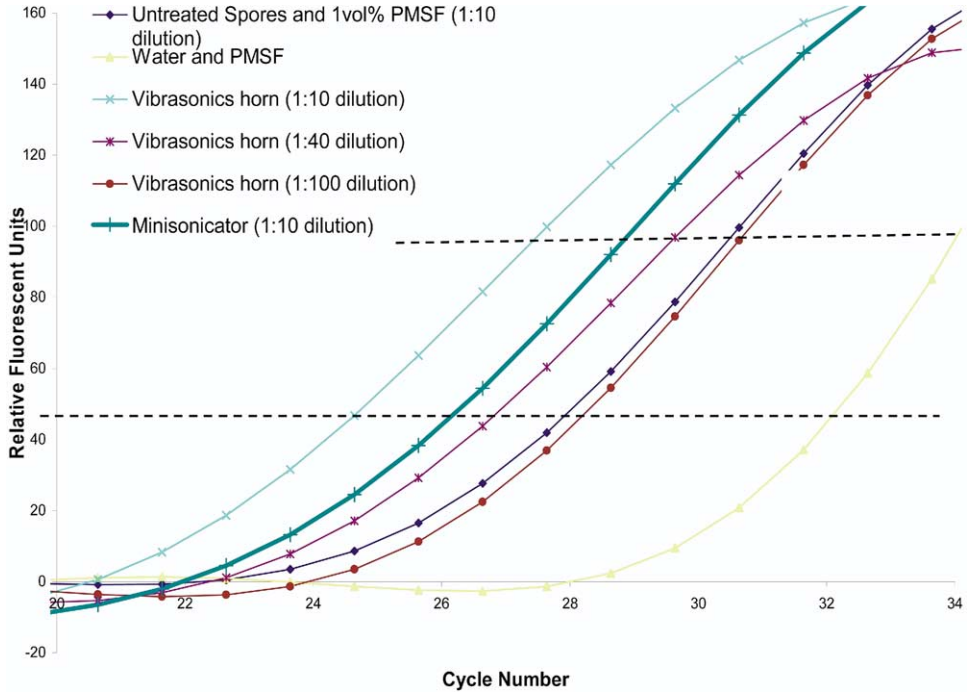

Fig. 5. Experiment 2 averaged real-time PCR (RTPCR) fluorescence signals of positive controls, negative controls and spores treated with the minisonicator. The Ct_{low} cut-off at 40 relative fluorescence units and Ct_{high} cut-off at 100 relative fluorescence units are clearly outlined.

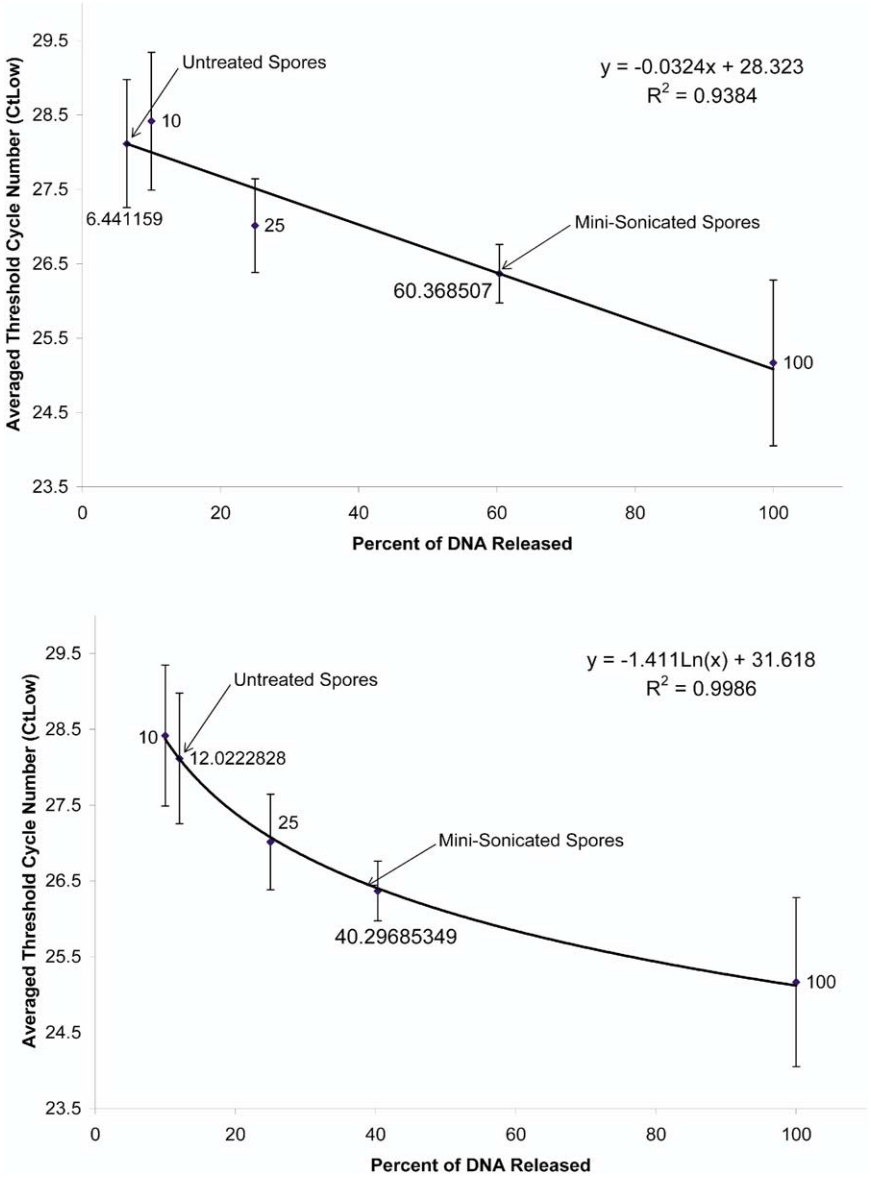

Fig. 6. Estimation of percent DNA made available using (a) Linear and (b) Logarithmic models. Ct_{low} of positive control serial dilutions 1:10, 1:40 and 1:100 from Fig. 5 are plotted vs. their respective concentrations and curve-fitted to produce a mathematical relation used to determine the percent of available DNA for minisonicated and untreated spores. Concentrations normalized so that the 1:10 dilution corresponds to 100% lysis.

To assess the effect of PMSF on untreated spores and the effect of flow on both positive and negative controls, we used two-tailed heteroscedastic *t*-testing. We compared the Ct_{low} and Ct_{high} of eight data points of PMSF-treated spores with untreated spores. We also compared samples that had flowed through the channel with spores that had not flowed through the channel.

Treatment time LD50

For the HL60 eukaryotic cell data at maximum transducer power (21 dBm) collected either *via* hemacytometry or FACS, we multiplied the treatment time (1.35 s) by 50 and divide it by the percent of cells killed to produce the treatment time LD_{50} (TLD_{50}). We performed the same calculation for the RTPCR data at 22 dBm with the appropriate treatment time (13.5 s).

RESULTS

Eukaryotic HL-60 results

The *t*-test comparison between HL-60 cells that had passed through the channel and controls that had not, in

terms of FS10 membrane damage and PI uptake, as well as in terms of FS94 membrane damage and PI uptake, yielded t values of 0.878, 0.217, 0.878 and 0.618, respectively. These t values were significant on the 0.05 level and demonstrated that mere flow of the HL-60 cells did not lyse the HL-60 cells, or even induce partial membrane structural damage that would manifest with increased trypan-blue uptake.

Hematocytometry data (Figs. 7 and 8; Table 1) revealed a near-linear decrease in the viability of intact HL-60 cells with increasing power applied to the minisonicator. The untreated control baseline rested at 10.2 ± 2.8% of the cells being trypan-blue positive (5.77×10^5 cells/mL alive, 6.44×10^4 cells/mL dead). At 15 dBm, a larger percentage of cells had compromised membranes, with 16.3% ± 0.7% being trypan-blue positive (2.48×10^5 cells/mL alive, 4.83×10^4 cells/mL dead). At 21 dBm, this value climbed to 75.9% ± 3.5% (5.83×10^4 cells/mL alive, 1.75×10^5 cells/mL dead). The power LD_{50} (PLD_{50}) was approximately 19.4 dBm. Because the cells flow at 50 μL/min and each cell spends 1.35 s under the transducers, we can calculate the time LD_{50} (TLD_{50}), which, at 22 dBm, equals 0.89 s of sonication treatment.

A parallel trend emerges when we plot the FACS FSC vs. SSC data gated at both FS10 and FS94 side-by-side to the hemacytometer data (Fig. 7). For FS10, the percent of viable cells was reduced from 80.2% ± 15.8% at 15 dBm to 18.0% ± 10.2% at 21 dBm, as shown in Table 1. In the case of FS94, we found 87.0% ± 3.8% of the cells alive at 15 dBm, which was reduced to 26.1% ± 12.8% alive at 21 dBm, as shown in Table 1. The hypotheses that the number of cells alive was reduced and that the number of cells lysed was increased were accepted using a homoscedastic one-sided t-test (p values < 0.001). The PLD_{50} at a flow rate of 50 μL/min for FS10 was 18.9 dBm and, for FS94, 19.7 dBm. The TLD_{50}s at a power of 21 dB at FS10 and FS94 were 0.82 s and 0.91 s, respectively.

Negative controls gated at FS10 had 8.9% ± 1.9% of the total events PI positive. At 21 dBm, this number had climbed to 27.1% ± 6.1%. The respective values with FS94 were 9.0% ± 1.0% and 53.8% ± 18.1% (p value < 0.0001) (Table 1). Because the data have already been normalized by dividing by the negative control percent value, there are no positive or negative control baselines.

B. subtilis results

A comparison between a batch of sonicated spores that had passed through the channel and one that had not gave a t value of 0.126 for Ct_{low} and 0.169 for Ct_{high}. For untreated (no sonication) spores and untreated spores passed through the channel, the corresponding t values were 0.214 and 0.581. Similarly, the Ct_{low} and Ct_{high} for spores with and without PMSF were 0.8785 and 0.8021 for the second experiment and 0.7021 and 0.4563 for the third experiment. All eight t values were significant on the 0.05 level that was chosen for the test. This means there is much higher than 0.05 probability that treated and untreated samples came from the same population. Therefore, the means were indistinguishable and neither

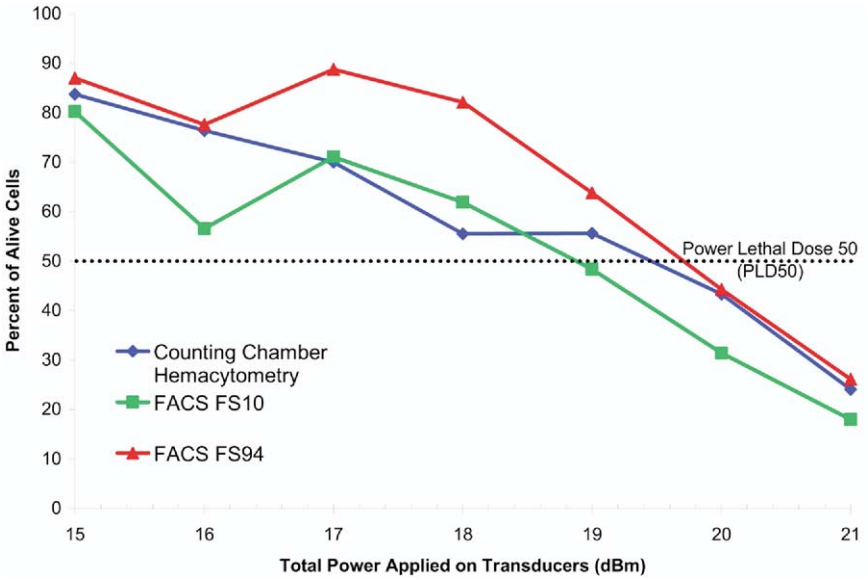

Fig. 7. Surviving percentage of HL-60 cells measured using FACS flow cytometry (FS10 and FS94) and percentage of intact trypan-blue negative cells measured using hematocytometry as a function of electrical power applied to the transducer.

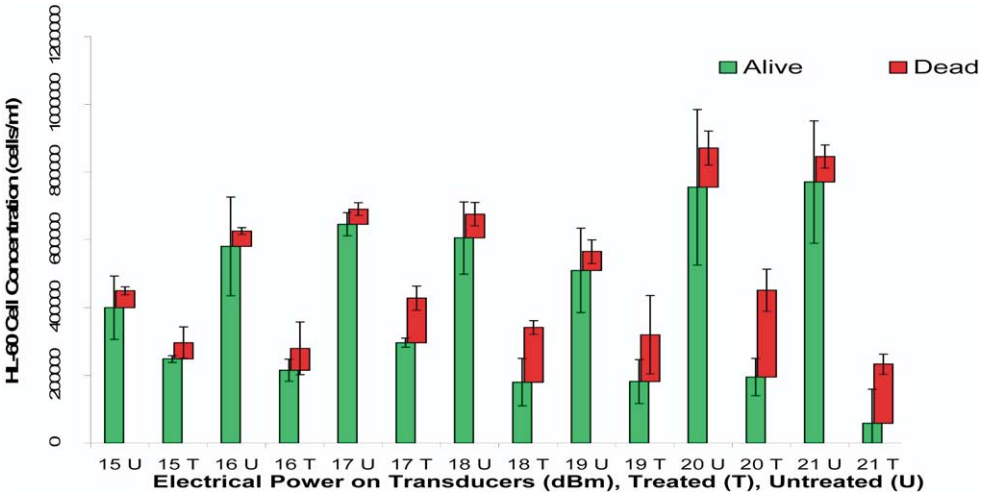

Fig. 8. Hemacytometer data showing concentrations of alive, trypan-blue-negative HL60 cells and dead, trypan-blue-positive HL60 cells. Samples before (U = untreated) and after treatment (T = treated) with the minisonicator at power levels between 15 and 21 dBm are shown.

flow nor the addition of PMSF had an appreciable effect on our controls by either inducing lysis or reducing the available sample.

The linear model of the first experiment was omitted because a linear curve-fit only poorly fitted the data ($R^2 = 0.80$). The linear model of the second experiment predicted 62.6% ± 9.5% lysis (p value < 0.0001), and that of the third experiment predicted 50.2% ± 4.4% (p value < 0.0001), shown in Table 2. The logarithmic model of the first experiment predicted 33.1% ± 3.3% lysis, the second experiment 43.3% ± 9.4% and the third 36.3% ± 6.7%, shown in Table 3. After averaging across all experiments, the linear model predicted a 56.3% ± 5.1% lysis, corresponding to a LD_{50} of 11.99 s. The logarithmic predicted a 37.5% ± 4.1% lysis, corresponding to an LD_{50} of 18.00 s. The lysing efficiency/acoustic intensity was 56.3%/1.11 W cm^{-2}. This corresponds with this treatment to 56.3%/1.50 W cm^{-2} s^{-1}. The results are summarized in Tables 2 and 3.

DISCUSSION

We began our experiments with HL-60 cells to get an estimate of the minisonicator's performance with a sample with mechanical rigidity (area compression modulus, K_A) similar to that of the majority of cells used in a modern bio lab (Boal 2002). Hemacytometry and FACS cytometry presented a combination of a well-established and a high-precision quantification method.

For the second part of the experiment, we chose *B. subtilis* because it is a cellular sample that is considered to be hard to lyse. It is also the organism of choice among researchers investigating sonication; thus, lending itself to comparison across studies (Belgrader et al. 1999). As a detection method, RTPCR measures available DNA, which correlates with sonication-induced rupture of the spore coat that allowed the DNA to leak outside the spores. It is also meaningful to use RTPCR because the subsequent step after sonication in a unified detection system would be PCR, to make the quantification as direct as possible to the application.

No comprehensive study is available on threshold pressures required to lyse spores and cells. Studies of bioeffects commonly use human or bovine erythrocytes or *B. subtilis* as cell and spore models. Ultrasound, either in the 20 to 40 kHz or in the 1 to 5 MHz range, is commonly applied and lysing thresholds in the 60 to 100

Table 1. Eukaryotic HL60 cells before and after treatment with the minisonicator

	10.2% ± 2.8%		75.9% ± 3.5%	
Trypan-blue-positive	FS10	FS94	FS10	FS94
Undamaged cells	100%	100%	18.0% ± 10.2%	26.1% ± 12.8%
Percent PI positive	8.3% ± 1.9%	9.0% ± 1.0%	27.1% ± 6.1%	53.8% ± 18.1%

Results collected using hematocytometry to count trypan-blue-positive (membrane compromised) cells and FACS flow cytometry gated at FS10 and FS94.

Table 2. *B. subtilis* RTPCR sonication experimental results interpreted with the linear model

	Ct_{low}	Ct_{high}	Average
Experiment 3	50.79% ± 4.70%	49.58% ± 7.10%	50.16% ± 4.42%
Experiment 2	60.37% ± 12.13%	64.55% ± 13.81%	62.62% ± 9.53%
Linear model average	–	–	56.32% ± 5.11%

Ct_{Low} and Ct_{High} of each experiment are averaged using Matlab to bootstrap the data. All experiments within the same model are averaged in a similar fashion.

kPa range with 10 to 60 s sonication times are cited (Chandler et al. 2001; Taylor et al. 2001; Miller et al. 1999). Comparison of reported results is, however, difficult, because no standardized procedure is used. A good example (Chandler et al. 2001) cites thresholds without beads for 10^8 colony-forming units (cfu)/mL of *B. subtilis* cells as 67 kPa for 12 s at 1.4 MHz, with 5 μL/ min flow and of *B. globgii* spores as 0.4 MPa for 2 to 9 s at 1 MHz, with 5 μL/ min flow. With 0.26 MPa pressure, the threshold is 62 s at 1.4 MHz, with 1 μL/ min flow. A TLD_{50} value of 1 s at 3.5 MHz and 0.3 MPa, with no beads for erythrocytes, has been reported (Kawai and Iino 2003). Another reference cites 21% lysis with 12 s of treatment in a continuous flow device (Chandler et al. 2001) and a third one, almost complete lysis (99.9%) with a 30 s treatment of a 100 μL sample in batch mode sonication (Belgrader et al. 1999).

A trade-off exists between flow rate and lysing efficiency that reflects on the choice of treatment time. Assuming a minimum intensity level, the longer the treatment time, the larger the lysed fraction of a population and the smaller the group of cells/spores that are not lysed (Miller 1987). On the other hand, the lower the flow rate, the lower the throughput of the lysing block in the PCR chain, which might reduce the response time of the instrument. The flow rate was, therefore, chosen so that it provided a throughput comparable with existing devices (Chandler et al. 2001) and a treatment time comparable with those reported earlier (Miller 1987).

The main concern with the PCR measurements was to ensure that lowered Ct values were caused by the presence of lysed spores rather than from impurities in the channel, extraneous DNA or amplification efficiency changes. Theory predicts a 0.73 cycle separation per 10-fold dilution with 12 amplifying sites. We measured a separation of 3.5 cycles. The discrepancy should not, however, have a deleterious impact on this research because we always compared a sonicated sample with the reference samples and only assumed that the amplification efficiency was the same. The amplification efficiency is determined by several factors, such as thermal cycler performance, changes in reagent formulation, degradation of target DNA and presence of PCR inhibitors (*e.g.*, detergents and proteins) (Chandler 1998). We tried to avoid these systematic errors by analyzing unsonicated and sonicated samples in a "blinded" fashion in one batch. This effectively reduces the systematic errors to random errors or to small trend shifts. Other errors (*e.g.*, pipetting errors, dilution errors, cell/spore clogging and adhesion) manifest themselves as an increased coefficient of variation for Ct values or complete failure to produce any RTPCR fluorescence signal. The impact of these errors was reduced by making use of very modest percent trimmed averages, which are justified by the large number of available parallel RTPCR data.

Bacterial spores carry extracellular DNA attached to their spore coat (Belgrader et al. 1999; Chandler et al. 2001), which causes a systematic reduction in Ct value, but which does not affect the change in threshold value, δCt. To simulate realistic field conditions, we carried out the RTPCR analysis of sonicated spores without first performing a wash (*e.g.*, with 10% sodium hypochlorite) to remove this extracellular DNA. As anticipated, this omission of the prewash made our negative controls appear sooner (24 vs. 32 in Belgrader et al. 1999 and 37 in Taylor et al. 2001) than those of researchers using an

Table 3. *B. subtilis* RTPCR sonication experimental results interpreted with the logarithmic model

	Ct_{low}	Ct_{high}	Average
Experiment 3	33.46% ± 3.67%	32.51% ± 5.36%	36.31% ± 6.65%
Experiment 2	40.30% ± 11.83%	46.07% ± 15.18%	43.31% ± 9.42%
Experiment 1	38.63% ± 11.24%	33.46% ± 7.34%	33.09% ± 3.34%
Logarithmic model average	–	–	37.49% ± 4.09%

Ct_{low} and Ct_{high} of each experiment are averaged using Matlab to bootstrap the data. All experiments within the same model are averaged in a similar fashion.

initial wash step. By comparing our results with a positive control, we see that we released 54% of all DNA that could have been released using traditional spore disruption methods. Our results from Tables 2 and 3 indicate a coefficient of variation of 10%, which is comparable with that of (*e.g.*, Ibrahim et al. 1998) at 9%. However, we cannot yet make a quantitative argument about how much intracellular DNA is made available through the minisonication, or how many PCR cycles the minisonicator saves us compared with existing lysing methods.

The current opinion among researchers involved in cell sonication tends to be that inertial cavitation, with a threshold of 1 W/cm^2, is the key cell lysis mechanism within the 20- to 2000-kHz frequency range (Feril et al. 2003). Our results indicate, however, that cell lysing also can be performed without relying on inertial cavitation. Our device operates in the 380-MHz range, which makes cavitation unlikely. Yet, the minisonicator accomplishes its intended function, hinting toward other noncavitational mechanisms as primary causes of cell disruption.

Sonication is known to produce short DNA fragments in the range of 100 to 500 base pairs (Picard et al. 1992), so we designed our primer pairs to replicate a 131 base pairs long sequence. To increase sensitivity, the sequence targeted corresponds to part of a structural RNA gene with 12 copies in the genome. This bears the risk of reducing specificity resulting in false-positives if aseptic conditions are not maintained. However, our negative water controls appear six cycles after the positive controls, corresponding to a 1% DNA concentration, negating this possibility.

Partial spore disruption may result in DNA release. We assume that percent of DNA made available correlates directly to lysis fraction because, for the purposes of an integrated genetic screening end product, whatever DNA is available will be detected, regardless of complete or partial spore lysis. A partial release of DNA is not very problematic either, because we were only interested in the capability to release, in part or fully, the DNA in the spores present in the sample.

The temperature increase observed in the channel makes it difficult to determine the lysing mechanism because, even though *B. subtilis* spores are impervious to 85°C heat (Kuske et al. 1998), erythrocytes have been lysed at 55°C (Kawai and Iino 2003), which is lower than the 70°C measured in the channel. If DNA release is the sole goal, then the lytic mechanism might be of less significance as long as DNA is released. However, to improve the system, it is necessary to understand the lysing mechanism, which makes it important to be able to separate the thermal and mechanical mechanisms. This may, perhaps, be done by comparing resistive heating results with ultrasonic lysing producing the same temperature.

Our results confirm that the minisonicator can disrupt 77.5% of the eukaryotic HL-60 cells at flow rates of 50 μL/min. At 5 μL/min, we lysed 54% of the *B. subtilis* spores. The fraction of the cells lysed with a particular method depends, however, on the method used, the type, size and concentration of the cells in the sample (Kuske et al. 1998). This means that complete lysing may not be obtainable for all pathogens with a certain device.

Current laboratory instruments, such as the BioRad iCycler used for this experiment, perform RTPCR on 10-μL samples. Our minisonicator needs 120 s to process such volumes. However, in the microfluidic realm, PCR chip researchers quote sample volumes of 0.280 μL (Chandler et al. 2001) that translate into 3.4 s sonication times with our device. Taking both cases into account, we believe that our device could be used for macrofluidic applications, especially when combined with other microfluidic elements.

The current device and protocol have been tested on a limited number of cell types and bacterial strains. Hence, device specifications need to be obtained for a variety of cell types and bacterial strains.

SUMMARY

We have demonstrated a novel microfluidic minisonicator that can, without physical or chemical pretreatment, disrupt eukaryotic HL-60 cells and *B. subtilis* vegetative spores, in a space- and energy-efficient manner. In the future, we hope to incorporate this lysing block into a variety of "lab-on-a-chip" implementations.

Acknowledgements—The authors gratefully acknowledge Prof. Pat Jones and her laboratory for their help with the hemacytometry and FACS. They also thank Prof. Rick Myer, his laboratory and, in particular, Jim Noonan for their help with the RTPCR part of this experiment. They thank Sanders Chong for his gene fragment mapping algorithm. This work was supported by DARPA's Bioflips program. Dr. Hæggström acknowledges the Wihuri-Foundation and the Academy of Finland for financial support.

REFERENCES

Andersson H, van den Berg A. Microfluidic devices for cellomics: A review. Sens Actuators A Phys 2003;B92(3):315–325.

Belgrader P, Elkin CJ, Brown SB, et al. A reusable flow-through polymerase chain reaction instrument for the continuous monitoring of infectious biological agents. Anal Chem 2003;75(14):3446–3450.

Belgrader P, Hansford D, Kovacs GTA, et al. A Minisonicator to rapidly disrupt bacterial spores for DNA analysis. Anal Chem 1999;71:4232–4236.

Boal D. Mechanics of the cell. 1st ed. New York: Cambridge University Press; 2002:343–348.

Chandler DP. Redefining relativity: Quantitative PCR at low template concentrations for industrial and environmental microbiology. J Ind Microbiol Biotechnol 1998;21:128–140.

Chandler DP, Brown J, Bruckner-Lea CJ, et al. Continuous spore disruption using radially focused, high-frequency ultrasound. Anal Chem 2001;73:3784–3789.

Chen WS, Brayman AA, Matula TJ, Crum LA. The pulse length-dependence of inertial cavitation dose and hemolysis. Ultrasound Med Biol 2003;29(5):725–737.

Feril LB, Kondo T, Zhao QL, et al. Enhancement of ultrasound-induced apoptosis and cell lysis by echo-contrast agents. Ultrasound Med Biol 2003;29(2):331–337.

Hianik T, Fajkus M, Sivak B, et al. The changes in dynamics of solid supported lipid films following hybridization of short sequence DNA. Electroanalysis 2000;12(7):495–501.

Ibrahim MS, Lofts RS, Jahrling PB, et al. Real-time microchip PCR for detecting single-base differences in viral and human DNA. Anal Chem 1998;70(9):2013–2017.

Inglesby TV, Henderson DA, Bartlett JG, et al. Anthrax as a biological weapon. J Am Med Assoc 1999;281(18):1735–1745.

Ivanova N, Sorokin A, Anderson I, et al. Genome sequence of Bacillus cereus and comparative analysis with Bacillus anthracis. Nature 2003;423(6935):87–91.

Jagannathan H, Yaralioglu GG, Ergun AS, Degertekin FL, Khuri-Yakub BT. Micro-fluidic channels with integrated ultrasonic transducers. Proc IEEE Ultrason Sympos 2001;2:859–862.

Jagannathan H, Yaralioglu GG, Ergun AS, Khuri-Yakub BT. Acoustic heating and thermometry in microfluidic channels. In: Proceedings of MEMS 2003 conference, Kyoto, Japan. 2003a:474–477.

Jagannathan H, Yaralioglu GG, Ergun, AS, Khuri-Yakub BT. An implementation of a microfluidic mixer and switch using micromachined acoustic transducers. In: Proceedings of MEMS 2003 conference, Kyoto, Japan. 2003b:104–107.

Janosi IM, Kessler JO, Horvath VK. Onset of bioconvection in suspensions of Bacillus subtilis. Phys Rev E Stat Phys Plasmas Fluids Relat Interdiscip Topics 1998;58(4):4793–4800.

Kawai N, Iino M. Molecular damage to membrane proteins induced by ultrasound. Ultrasound Med Biol 2003;29(4):609–614.

Khuri-Yakub BT, Smits JG, Barbee T, Reactive magnetron sputtering of ZnO. J Appl Phys 1981;52:4772–4774.

Kino GS. Acoustic waves: Devices, imaging, and analog signal processing. Englewood Cliffs, NJ: Prentice-Hall, 1987:41.

Knight J. Microfluidics: Honey, I shrunk the lab. Nature 2002;418: 474–475.

Kopp MU, de Mello AJM, Manz A. Chemical amplification: Continuous-flow PCR on a chip. Science 1998;280:1046–1048.

Kuske CR, Banton KL, Adorada DL, et al. Small-scale DNA sample preparation method for field PCR detection of microbial cells and spores in soil. Appl Environ Microbiol 1998;64(7):2463–2472.

Lagally ET, Medintz I, Mathies RA. Single-molecule DNA amplification and analysis in an integrated microfluidic device. Anal Chem 2001;73:565–570.

Miller DL. A review of the ultrasonic bioeffects of microsonication, gas-body activation, and related cavitation-like phenomena. Ultrasound Med Biol 1987;13(8):443–470.

Miller DL, Bao S, Morris JE. Sonoporation of cultured cells in the rotating tube exposure system. Ultrasound Med Biol 1999;25(1): 143–149.

Miller DL, Dou C, Song J. DNA transfer and cell killing in epidermoid cells by diagnostic ultrasound activation of contrast agent gas bodies *in vitro*. Ultrasound Med Biol 2003;29(4):601–607.

More MI, Herrick JB, Silva MC, Ghiorse WC, Madsen EL. Quantitative cell lysis of indigenous microorganisms and rapid extraction of microbial DNA from sediment. Appl Environ Microbiol 1994; 60(5):1572–1580.

Patolsky F, Lichtenstein A, Willner I. Electronic transduction of DNA sensing processes on surfaces: Amplification of DNA detection and analysis of single-base mismatches by tagged liposomes. J Am Chem Soc 2001;123:5194–5205.

Picard C, Ponsonnet C, Paget E, Nesme X, Simonet P. Detection and enumeration of bacteria in soil by direct DNA extraction and polymerase chain-reaction. Appl Environ Microbiol 1992;58(9): 2717–2722.

Read TD, Peterson SN, Tourasse N, et al. The genome sequence of Bacillus anthracis Ames and comparison to closely related bacteria. Nature 2003;423:81–86.

Rothery P, Newton I, Dale L. Testing for density dependence allowing for weather effects. Oecologia 1997;112(4):518–523.

Sun K, Yamaguchi A, Ishida Y, Matsuo S, Misawa H. A heater-integrated transparent microchannel chip for continuous-flow PCR. Sens Actuators A Phys 2002;B84:283–289.

Taylor MT, Belgrader P, Furman BJ, et al. Lysing bacterial spores by sonication through a flexible interface in a microfluidic system. Anal Chem 2001;73:492–496.

Thewes R, Hofmann F, Frey A, et al. Sensor arrays for fully-electronic DNA detection on CMOS. Solid-state circuits conference, digest of technical papers ISSCC. IEEE Int 2002;1:350–473.

Umek RM, Lin SW, Vielmetter J, et al. Electronic detection of nucleic acids: A versatile platform for molecular diagnostics. J Mol Diagn 2001;3(2):74–84.

van Duijn MM, van der Zee J, van Steveninck J, van den Broek PJA. Ascorbate stimulates ferricyanide reduction in HL-60 cells through a mechanism distinct from NADH-dependent plasma membrane reductase. Biol Chem 1998;273(22):13415–13420.

Yaralioglu GG, Wygant IO, Marentis TC, Khuri-Yakub BT. Ultrasonic mixing in microfluidic channels using integrated transducers. Anal Chem 2004;76:3694–3698.

Zeng S, Chen C, Mikkelsen JC, Santiago JG. Fabrication and characterization of electroosmotic micropumps. Sens Actuators A Phys 2001;B79(2–3):107–114.